

Simulation of Crystallization Kinetics and Morphology During Nonisothermal Crystallization in Short Fiber Reinforced Composites

Chunlei Ruan, Jie Ouyang

Department of Applied Mathematics, Northwestern Polytechnical University, Xi'an, 710129, People's Republic of China

Received 7 July 2010; accepted 20 March 2011

DOI 10.1002/app.34565

Published online 19 August 2011 in Wiley Online Library (wileyonlinelibrary.com).

ABSTRACT: Computer simulation for the nonisothermal crystallization of short fiber reinforced composites is presented. The pixel coloring technique is implemented to the study of crystal morphology evolution as well as the crystallization kinetics. A parametric study is used to explore the influences of thermal conditions and fibers on the crystallization in the reinforced system. We particularly focus on the roles of cooling rate, initial temperature, nucleation density on fibers, fiber content, fiber length, and fiber diameter. The results indicate that cooling rate is a significant factor to the crystallization kinetics as well as the morphology. The initial temperature only affects the crystallization kinetics and has minor impact on the morphology. The additional fibers have a dual effect on

the crystallization. They depress the crystallization rate by hindering the spherulitic growth and accelerate the crystallization rate by providing nucleation sites. The constraining effect is mainly dependent on fiber content, whereas the enhancing effect is mainly determined by fiber surface and fiber nucleation density as well as surface nucleation mode. Present results are hoping to give more insight about the crystallization in short fiber reinforced composites and be more helpful to the industrial application. © 2011 Wiley Periodicals, Inc. *J Appl Polym Sci* 123: 1584–1596, 2012

Key words: crystallization; morphology; simulations; nonisothermal; composites.

INTRODUCTION

Short fiber in the production of polymer composites for high-technology applications is increasing rapidly because of their good mechanical, thermal, and electrical properties. Short fiber, in particular, have the additional advantage of being able to be processed using conventional processing techniques, such as extrusion and injection molding. Studies related to the kinetics of crystallization and the morphology are of great importance in the manufacture processing, because of the fact that the resulting physical properties are strongly dependent on the morphology formed and the extent of crystallization occurring during processing.^{1,2}

In the fiber reinforced system, the classical equation of crystallization kinetics is unable to describe the conversion of polymer melt into spherulites.^{3–8} This is mainly due to the fact that, on the one hand, the spherulite growth fronts is not unconstrained

because of the exist of fibers; on the other hand, the surface nucleation makes the overall nucleation process nonrandom. Some researchers^{4,5} have tried to derive the analytical models to take into account the roles of long fibers. However, other than the simplest case of isothermal with athermal nucleation; none of the analytical model is found in the literature to describe the crystallization of reinforced composites. Numerical simulation is another efficient tool in the prediction of crystallization kinetics and morphology in fiber reinforced composites. Numerical modeling of isothermal crystallization in systems reinforced with long fibers was conducted by Mehl and Rebenfeld,^{6–8} Krause et al.,³ and Piorkowska.⁵ In those models, either the instantaneous or spontaneous nucleation in polymer bulk was assumed whereas the nucleation on fiber surfaces was treated as instantaneous. Overall, previous studies of crystallization in fiber reinforced system are concentrated on the simple isothermal case, moreover, the fibers are long and unidirectional.

Because the manufactory usually contains the complex thermal history, nonisothermal case is more common in the real world. Several theoretical and numerical works have been devoted to the study of nonisothermal crystallization in the pure crystalline/semicrystalline polymer system. The theoretical models, including Nakamura^{9,10} and Kolmogorov

Correspondence to: J. Ouyang (jieouyang@nwpu.edu.cn).

Contract grant sponsor: Natural Sciences Foundation of China; contract grant number: 10871159.

Contract grant sponsor: National Basic Research Program of China; contract grant number: 2005CB321704.

model,¹¹ are the most representative ones. Both of them are based on the Avrami equation^{12–14} in the isothermal crystallization. In addition, the former one is based on the isokinetics, whereas the latter one is based on the morphology evolution of crystallization. Numerical studies of crystal morphology evolution in nonisothermal system have been carried out by Charbon and Swaminarayar,¹⁵ Huang and Kamal,¹⁶ and Chen and coworkers.¹⁷ They used the morphological method to model the polymer solidification.

Introducing fiber into polymeric material affects both the crystallization kinetics and morphology. Of course, the crystallization of the system is more complex and interesting than that of pure polymer.

In our previous work,¹⁸ we have presented a pixel coloring method in the simulation of isothermal crystallization for short fiber reinforced system and have explored the effects of fiber orientation, fiber surface nucleation density, fiber content, fiber size on the crystallization kinetics, and morphology. In this article, we will extend our simulation to the nonisothermal crystallization.

The objective of this article is twofold: first, to explore the effects of thermal condition, e.g., cooling rate, initial temperature, on the crystallization kinetics and morphology; second, to explore the characteristic of fiber, e.g., fiber surface nucleation density, fiber content, fiber size, on the crystallization in the nonisothermal reinforced system. It is worth mentioning that the effect of fiber orientation which is an intrinsic property of short fiber shall not be investigated as its effect on both morphology and crystallization kinetics is minor.¹⁸

COMPUTER MODELING AND SIMULATION

We investigate the nonisothermal crystallization, and a linear decrease of the temperature is assumed: $T = T_0 - c \times t$, where T_0 is the initial temperature, c is the cooling rate, and t is the time. We shall mention that this temperature equation is more related to the experimental processing.^{1,17,19,20}

Modeling the crystallization

In the crystalline/semicrystalline system, crystals follow the steps of nucleation, growth, and impingement. Once nucleated, spherulites grow at a rate of G in all available radial directions until impingement with the growth front of another spherulite or with a reinforcing fiber. Growth is stopped only in the radial direction at which impingement takes place and continues in all other radial directions until all possible materials are transformed. It should be mentioned that our simulation is at the spherulite level, the crystals contain both crystalline and the amor-

phous phase rather than purely crystalline structures. Therefore, it is independent of the degree of crystallinity within the semicrystalline phase of polymer.

This study is an extension of our previous work.¹⁸ Therefore, the model we used here is similar to that we used in the isothermal system. In our previous work,¹⁸ roles of polymer bulk and the fibers are defined separately: three variables, namely, rate of radial spherulitic growth $G(t)$, nucleation density in the polymer bulk $N_b(t)$, and time from onset of nucleation t are used to describe the neat polymer system; five variables, namely, nucleation density on fibers $N_f(t)$, fiber diameter d , fiber length l , number of fibers per area n_f , and fiber orientation angle θ are used to take into account the effect of fibers. Unlike the situation of isothermal crystallization, in the nonisothermal system, the values of $N_b(t)$, $N_f(t)$, and $G(t)$ should not be set to be constant and independent of time. They should be a function of temperature. Moreover, the definition of time t in the nonisothermal system is different from that in the isothermal case.

Different nucleation relations of N_b are reported, reviews of Pantanin et al.¹⁹ are helpful. Usually, scientists in modeling nucleation in realistic systems have been forced to use an empirical approach. They use the simple analytical relationship to fit the differential scanning calorimetry experimental data to obtain the empirical relationship between the spherulite density and the temperature. However, the empirical relationship may quite restrict depending on the conditions or materials. Here, we adopt the relations of nucleation density in the polymer bulk proposed by Pantanin et al.,^{19,21} and assume it to be a unique function of the supercooling temperature ΔT to get

$$\begin{aligned} N_b(t) &= N_b(T) = N_0 \exp[\varphi \Delta T] \\ &= N_0 \exp\{\varphi [T_m^0 - (T_0 - c \times t)]\} \end{aligned} \quad (1)$$

where $\Delta T = T_m^0 - T$ with T_m^0 being the equilibrium melting temperature, N_0 and φ are the empirical parameters. As we study the 2D problem, we shall convert the 3D of eq. (1) to a 2D spherulite density, and use the stereological relationship¹⁵

$$N_{2D} = 1.458(N_{3D})^{2/3} \quad (2)$$

The nucleation density on fiber surface is extremely complicated, and to date, none of the expression is found in the literature. For the sake of simplicity, we assume that the rate of nucleation per unit fiber surface is constant below the critical temperature T_c , namely,

$$\begin{aligned} \dot{N}_f(t) &= \dot{N}_f(T) = \begin{cases} 0 & T > T_c \\ \dot{N}_f & T \leq T_c \end{cases} \\ &= \begin{cases} 0 & t < (T_0 - T_c)/c \\ \dot{N}_f & t \geq (T_0 - T_c)/c \end{cases} \end{aligned} \quad (3)$$

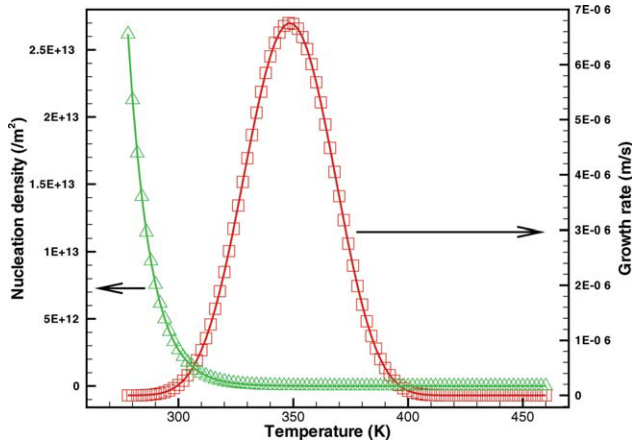


Figure 1 Relationship between temperature and nucleation density in the polymer bulk as well as growth rate. [Color figure can be viewed in the online issue, which is available at wileyonlinelibrary.com.]

Therefore, the nucleation density on fibers per unit fiber surface can be calculated by

$$N_f(t) = \dot{N}_f(t) \times [t - (T_0 - T_c)/c] \quad (4)$$

Other than the various kinds of relations of nucleation density in polymer bulk, the expression of spherulite growth rate is rare. Usually, it is assumed to be only a function of temperature and to follow the Hoffman-Lauritzen theory²²

$$\begin{aligned} G(t) = G(T) &= G_0 \exp\left[-\frac{U^*}{R_g(T - T_\infty)}\right] \exp\left(-\frac{K_g}{T\Delta T f}\right) \\ &= G_0 \exp\left[-\frac{U^*}{R_g(T_0 - c \times t - T_\infty)}\right] \\ &\quad \times \exp\left(-\frac{K_g}{(T_0 - c \times t)[T_m^0 - (T_0 - c \times t)]f}\right) \end{aligned} \quad (5)$$

where G_0 and K_g are constants, U^* is the activation energy of motion, R_g is the gas constant, $T_\infty = T_g - 30$ (where T_g is the glass transition temperature), and $f = 2T/(T_m^0 + T)$.

We use the pixel coloring method presented in our previous work¹⁸ to capture the growth front of a population of spherulites and use the "minimal-time principle" to show the impingement to ensure that every pixel has the color of the first spherulite by which it is reached.

The addition of fibers makes our simulation more complicated. One shall first create the fibers in the computational region and determine the fiber surface points in the length direction with the help of technique presented in our previous work.¹⁸

The relative crystallinity in our study can be calculated by

$$\alpha = \frac{\text{number of cells that have been transformed/}}{\text{number of cells of polymer bulk}} \quad (6)$$

and the mean radius of each spherulite can be defined as

$$\bar{R} = \sqrt{S/\pi} \quad (7)$$

with S the area of the spherulite which can be calculated with the number of cells occupied by the spherulite and the cell size.

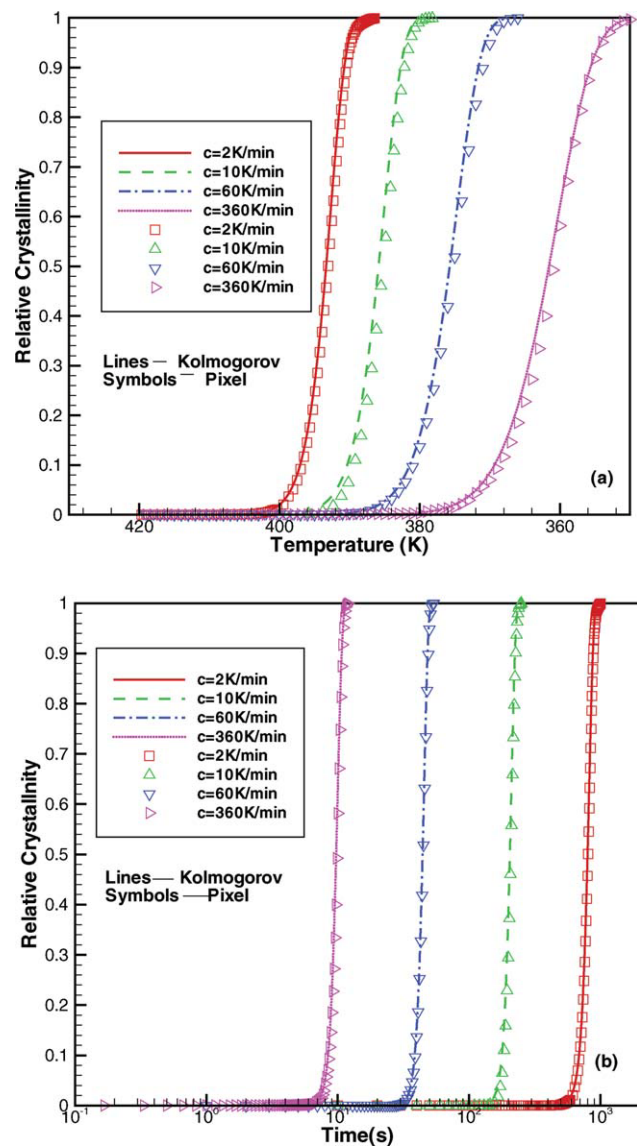


Figure 2 Comparison of relative crystallinity with different cooling rates, between Kolmogorov model and pixel coloring method (a) evolves with temperature (b) evolves with time. [Color figure can be viewed in the online issue, which is available at wileyonlinelibrary.com.]

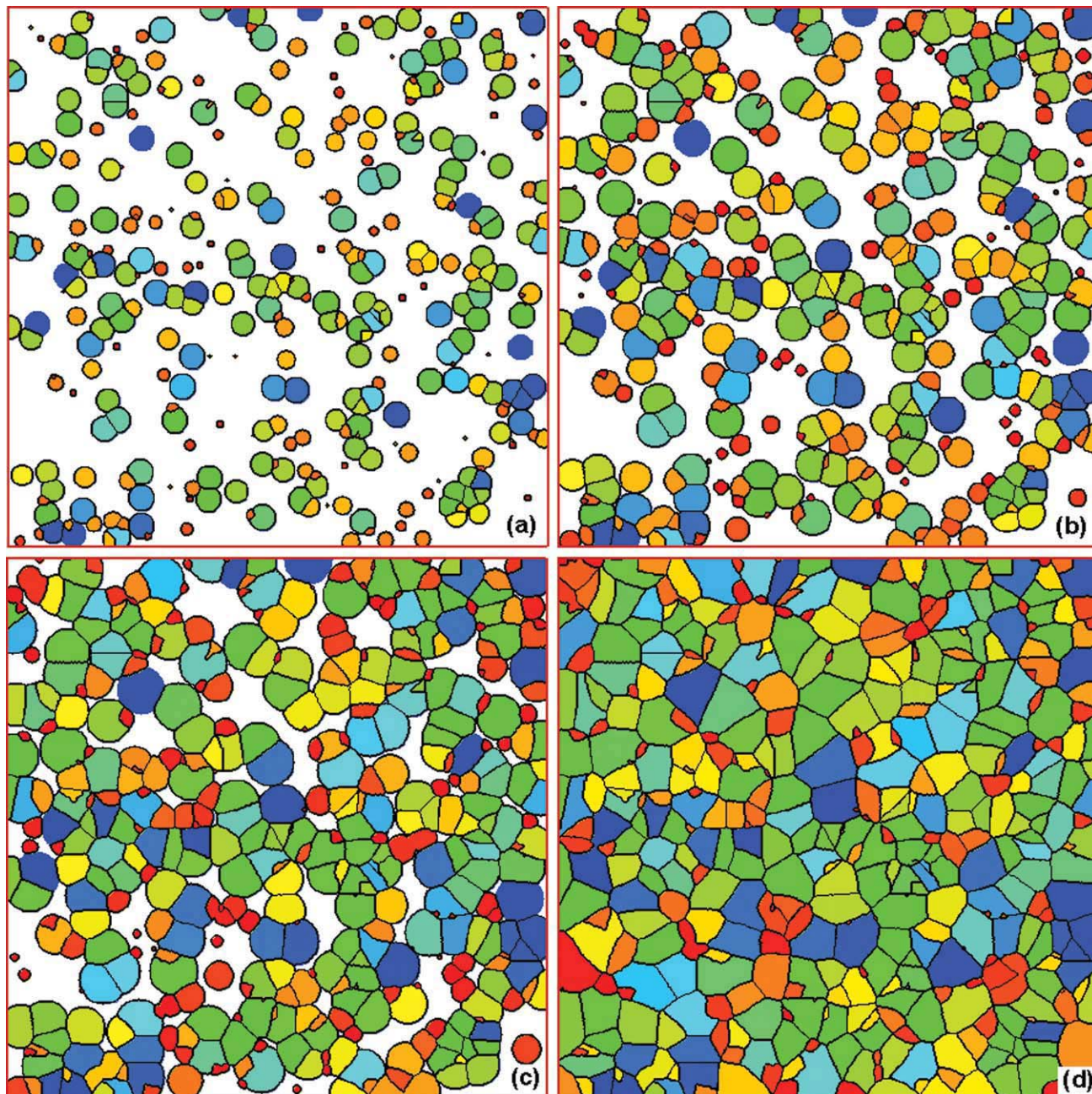


Figure 3 Evolution of crystal morphology in polymer system (a) $t = 199s$, (b) $t = 211s$, (c) $t = 221s$, and (d) $t = 251s$. [Color figure can be viewed in the online issue, which is available at wileyonlinelibrary.com.]

Kolmogorov model

In the nonisothermal polymer crystallization, Nakamura and Kolmogorov models are the most important ones in description of polymer crystallization kinetics. Despite of the fact that the Nakamura approaches do predict well in the nonisothermal crystallization kinetics, it has often been pointed out in the literature that the Nakamura's equation cannot reveal the details of the crystal morphology.¹⁹ These limits are overcome by considering the crystallization phenomenon as the Kolmogorov model does. Accordingly, Kolmogorov mode¹⁹

which describes crystallinity evolution accounting of the number of nuclei per unit volume and spherulitic growth rate can be applied. The corresponding equations are

$$\alpha = 1 - \exp(-\alpha_f) \quad (8)$$

$$\alpha_f = C_m \int_0^t \frac{dN(s)}{ds} \left[\int_0^t G(u) du \right]^m ds \quad (9)$$

where α_f is the fictive volume fraction, m is a dimensionality exponent, C_m is a shape factor, G is the

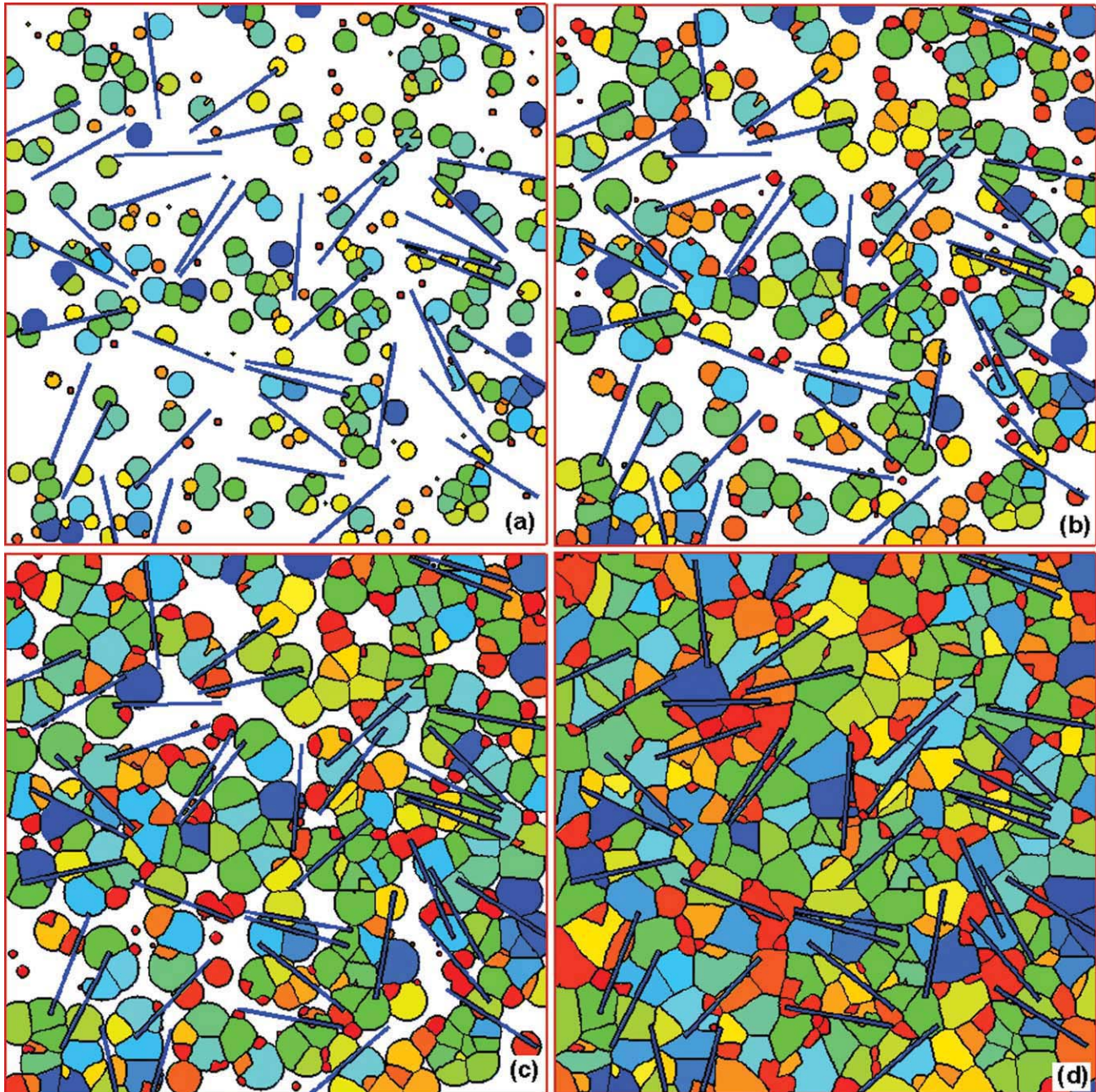


Figure 4 Evolution of crystal morphology in short fiber reinforced system with $N_f = 0/mm$ (a) $t = 199s$, (b) $t = 211s$, (c) $t = 221s$, and (d) $t = 251s$. [Color figure can be viewed in the online issue, which is available at wileyonlinelibrary.com.]

linear growth rate and N is the nucleation density. In our case, $m = 2$, $C_m = \pi$.

RESULTS AND DISCUSSION

Parameters and basic properties

Parameters used in the simulation are^{19,21}: $N_0 = 17.4 \times 10^6/m^3$, $\phi = 0.155$, $G_0 = 2.1 \times 10^{10} \mu m/s$, $U^*/R_g = 755 \text{ K}$, $K_g = 534858 \text{ K}^2$, $T_m^0 = 467 \text{ K}$, $T_g = 266 \text{ K}$, $T_c = 420\text{K}$, and $T_0 = 420\text{K}$. Unless otherwise stated, the fiber parameters are: $l = 200 \mu m$, $d = 8 \mu m$, and $n_f =$

$37.5/mm^2$. In the implement of this algorithm, the computational domain is considered as $1mm \times 1mm$, and the number of cells are 500×500 .

The relationship between the temperature and nucleation density in the polymer bulk N_b according to eqs. (1) and (2) as well as the spherulite growth rate G according to eq. (5) are shown in Figure 1. The nucleation density in the polymer bulk is a monotonous decreased function with the temperature. The lower temperature is, the larger nucleation density in the polymer bulk is. However, the growth rate is not a monotonous function: it takes on a first

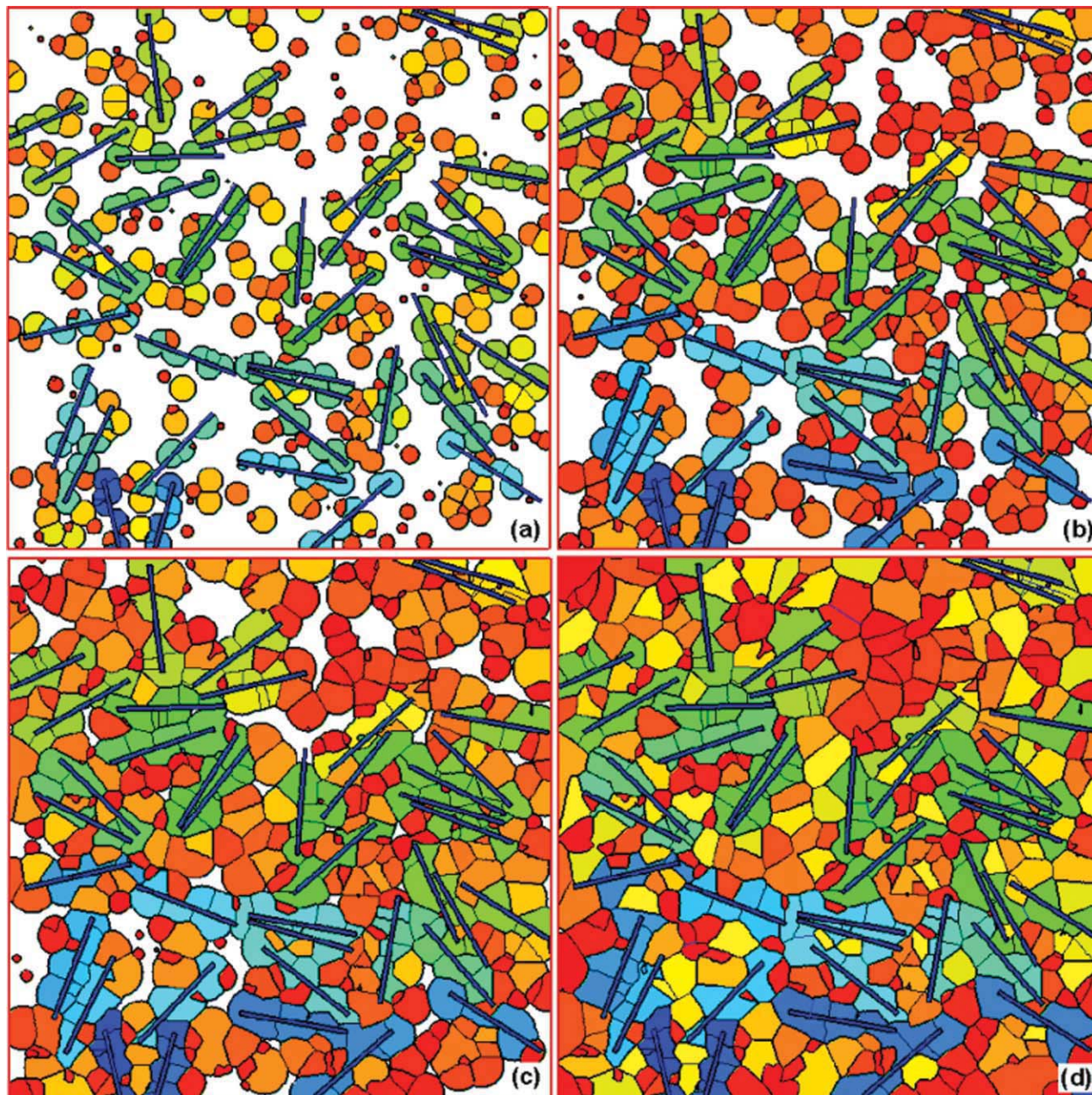


Figure 5 Evolution of crystal morphology in short fiber reinforced system with $N_f = 20/mm$ (a) $t = 190s$, (b) $t = 203s$, (c) $t = 215s$, and (d) $t = 248s$. [Color figure can be viewed in the online issue, which is available at wileyonlinelibrary.com.]

increase then decrease tendency when temperature decreases. The growth rate has a peak when the temperature approaches 350 K.

Validity of the simulation

To confirm the validity of our simulation, numerical results of crystallization kinetic data are compared with the data calculated with the Komlogrov model in the polymer system which is shown in Figure 2. As we can see that the numerical data shows fair agreement with the analytical data.

Therefore, the method presented here is valid and reliable. It is also notable that the increasing the cooling rate leads to an acceleration of the crystallization but a large range of temperature for the crystallization.

The morphology development of crystallization with cooling rate $c = 10K/min$ is shown in Figure 3. The white region is the polymer melt, whereas the colored region is the spherulitics. Different spherulitics are distinguished by different colors. These results are qualitatively similar to those obtained by Charbon and Rappaz²³ as well as Huang and

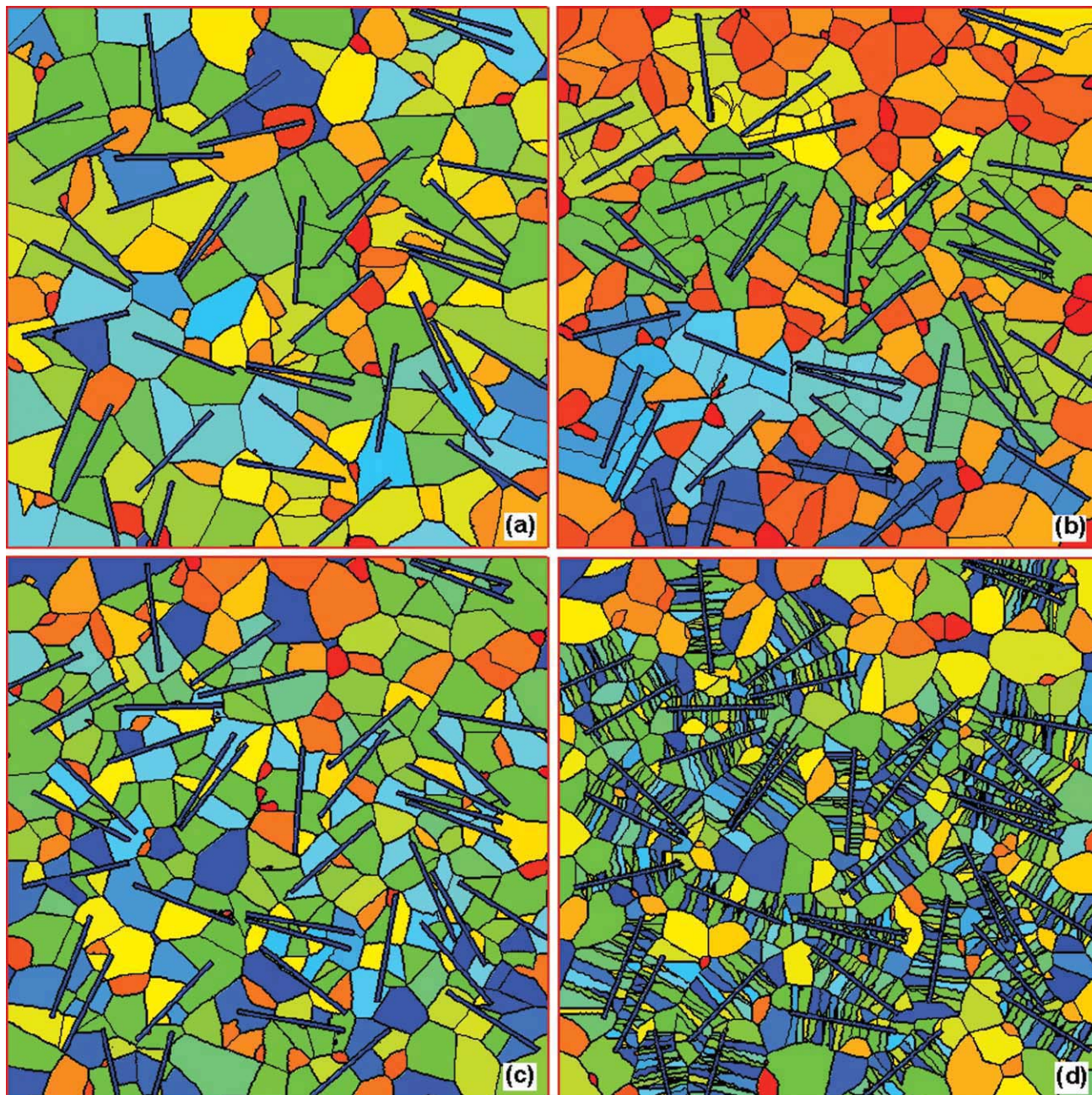


Figure 6 Crystal morphology with different N_f (or \dot{N}_f) in the case of $c = 2K/\text{min}$ (a) $N_f = 0/\text{mm}$ ($t = 937\text{s}$), (b) $N_f = 20/\text{mm}$ ($t = 901\text{s}$), (c) $\dot{N}_f = 1.2/\text{min}/\text{mm}$ ($t = 905\text{s}$), and (d) $\dot{N}_f = 12/\text{min}/\text{mm}$ ($t = 899\text{s}$). [Color figure can be viewed in the online issue, which is available at wileyonlinelibrary.com.]

Kamal.¹⁶ Hence, the morphology of the crystallization predicted here is also convincing. In the nonisothermal crystallization, nucleation sites form with the evolution of time (temperature), therefore, the distribution of spherulite size is much wider than isothermal case. In addition, the shape of grain boundaries is also different from the isothermal case: the boundaries between two neighboring spherulites are curved if they were nucleated at different times, and straight if they were nucleated at the same time.

Effects of fibers on the evolution of morphology

The evolution of crystal morphology of short fiber reinforced system with no extra nucleation sites on fibers is presented in Figure 4. Compared with the unreinforced system in Figure 3, the existence of fibers in Figure 4 hinders the spherulitics' growth front by an impingement mechanism.

The evolution of crystal morphology of short fiber reinforced system with instantaneous nucleation density $N_f = 20/\text{mm}$ on fibers is presented in

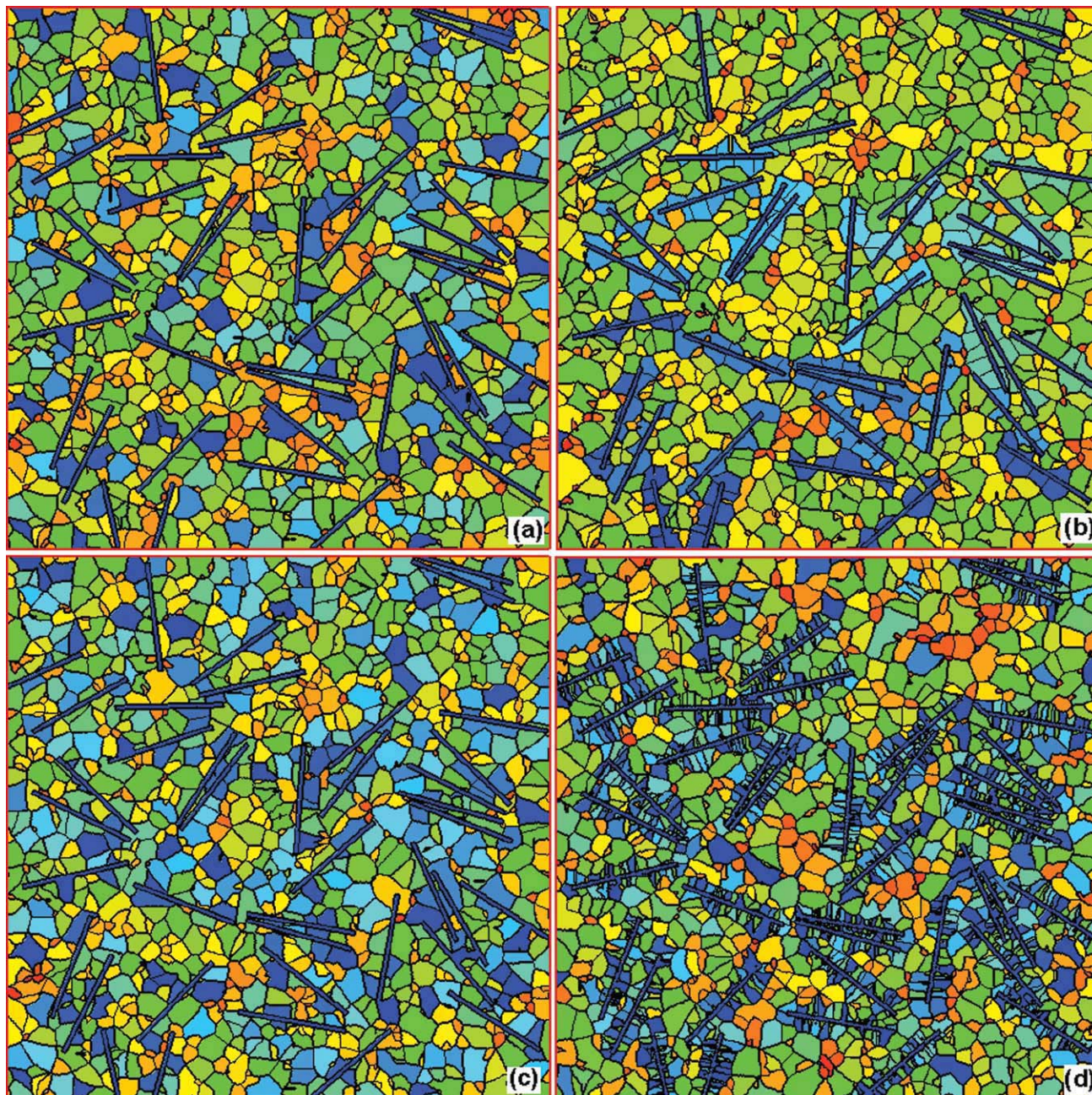


Figure 7 Crystal morphology with different N_f (or \dot{N}_f) in the case of $c = 60K/min$ (a) $N_f = 0/mm$ ($t = 55s$), (b) $N_f = 20/mm$ ($t = 52s$), (c) $\dot{N}_f = 20/min/mm$ ($t = 53s$), and (d) $\dot{N}_f = 200/min/mm$ ($t = 50s$). [Color figure can be viewed in the online issue, which is available at wileyonlinelibrary.com.]

Figure 5. Because of the additional nucleation sites on fibers, the morphology near the fibers takes on a significant difference. The highly oriented spherulites appear near the fiber surface. These regions of oriented spherulites, often referred to as transcrystalline regions,¹⁹ occur near fiber surfaces when the local fiber nucleation density is so large that spherulites are constrained by their neighbors to grow in a direction perpendicular to the fiber axis.

Effects of cooling rate and nucleation density on fibers

Figure 6 shows the crystal morphology with different nucleation density on fibers' surface. The cooling rate is $c = 2K/min$. We shall mention that the nucleation density on fibers in Figure 6(b,c) are very close, whereas the nucleation density on fibers in Figure 6(d) is almost nine times higher. As we can see from Figure 6(a,c,d), with the increase of N_f (or \dot{N}_f), the morphology of transcrystallinity becomes more

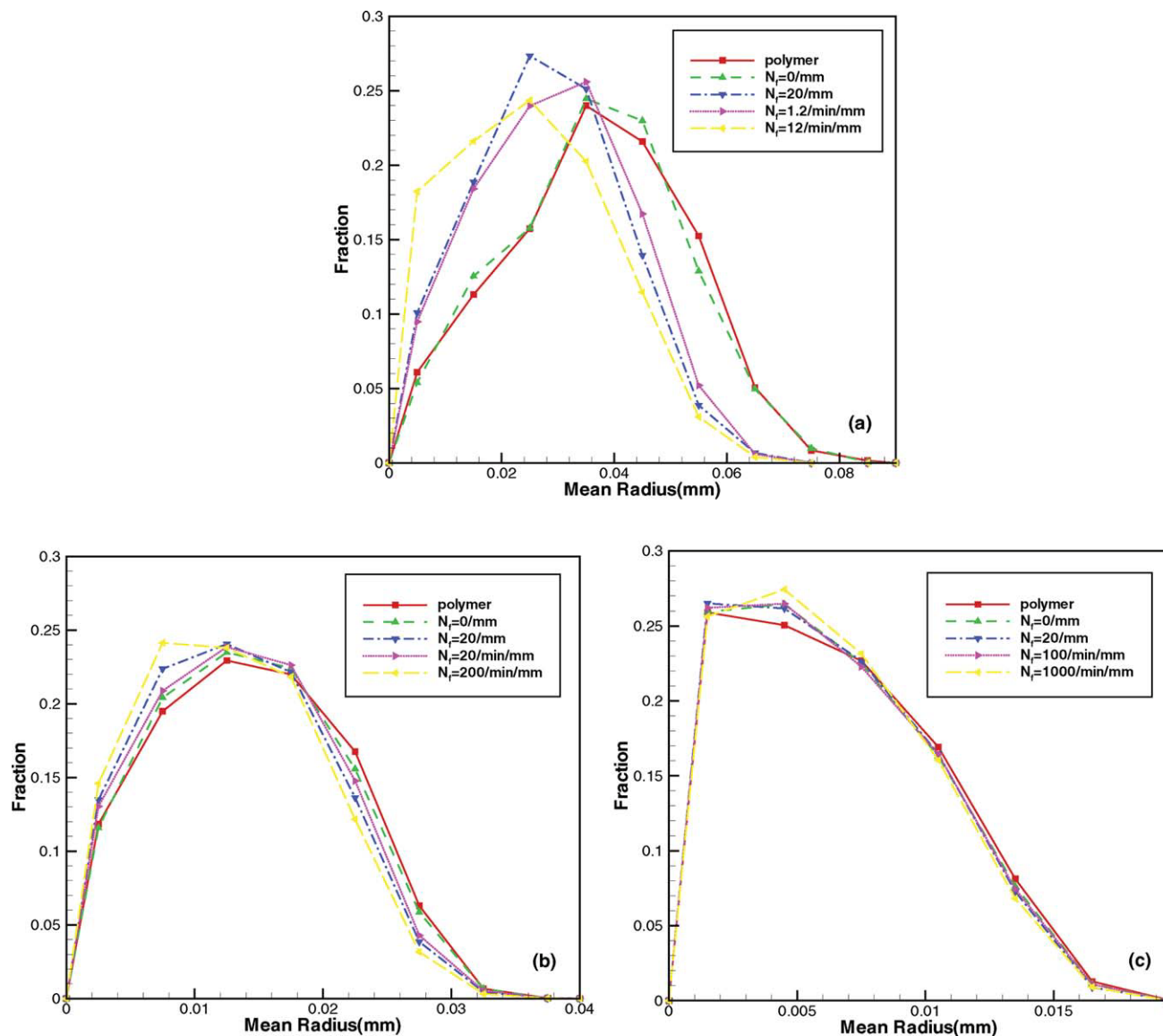


Figure 8 Effects of cooling rate on the mean radius (a) $c = 2K/min$, (b) $c = 60K/min$, and (c) $c = 360K/min$. [Color figure can be viewed in the online issue, which is available at wileyonlinelibrary.com.]

obvious. However, under the conditions of similar surface nucleation density, the instantaneous nucleation on fibers showing in Figure 6(b) leads to a more regular and larger transcrystalline region than that spontaneous nucleation in Figure 6(c). This phenomenon agrees with the numerical study by Mehl and Rebenfeld⁸ with long fibers. They claimed that the instantaneous nucleation should be viewed as the high nucleation rate limiting case of spontaneous nucleation to exhaustion.⁵

Figure 7 presents the results of morphology with $c = 60K/min$, in which the other parameters are the same as those in Figure 6. Compared with Figure 6, the mean size of spherulitics reduces in this higher cooling rate case. Moreover, the morphology of transcrystallinity becomes less obvious in this case.

Mean radius of spherulites are compared with different nucleation density on fiber surface. This is shown in Figure 8 where different cooling rate is also discussed. In the case of short fiber reinforced system, when no extra nucleation is considered on fiber surface ($N_f = 0/mm$), the mean radius of spherulites is less than that of the pure polymer due to the existence of fibers that cannot be transformed. With the increase of nucleation density (or rate) on fiber surface, the mean radius of spherulites in the polymer bulk decreases owing to the increase of transcrystallinity region. In addition, under the conditions of similar fiber surface nucleation density, due to the earlier nucleation and initiate growth, transcrystallinity region in the instantaneous nucleation ($N_f = 20/mm$) is larger than in spontaneous case [Fig. 8(a), $\dot{N}_f = 1.2/min/mm$; Fig. 8(b), $\dot{N}_f = 20/min/mm$; and

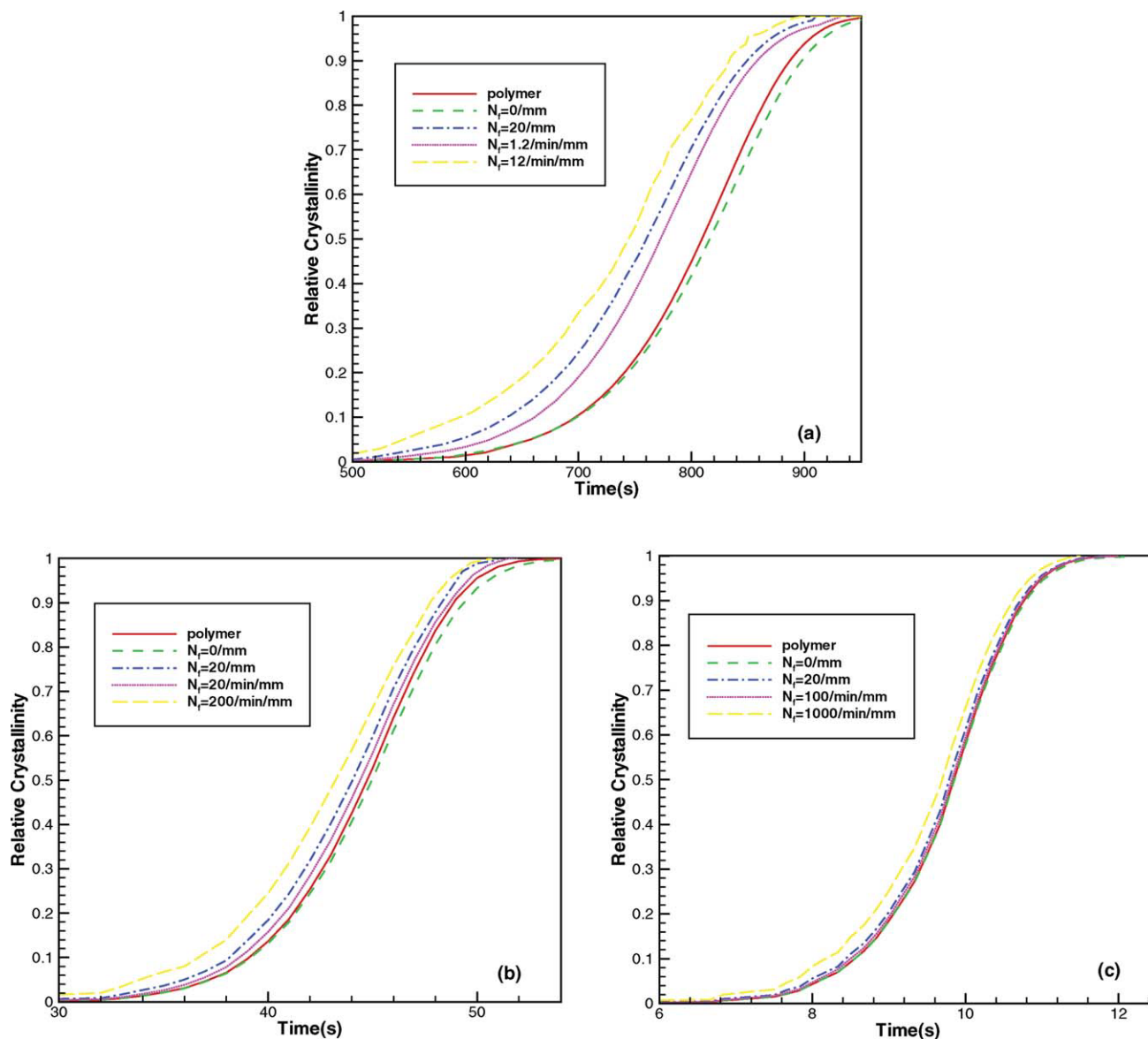


Figure 9 Effects of cooling rate on the crystallization kinetics (a) $c = 2\text{K/min}$, (b) $c = 60\text{K/min}$, and (c) $c = 360\text{K/min}$. [Color figure can be viewed in the online issue, which is available at wileyonlinelibrary.com.]

Fig. 8(c), $\dot{N}_f = 1000/\text{min/mm}$], therefore, corresponding mean radius is less than the latter one. The increase of cooling rate leads to a smaller value of mean radius of spherulites and also a less sound effect of nucleation density on fiber surface.

Corresponding crystallization kinetics is shown in Figure 9. In the fiber reinforced system, when no nucleation is added to the fiber surface, fibers hinder the spherulites growth front by an impingement mechanism, therefore, the crystallization rate is depressed. However, when fibers provide proper or a great many of surface nucleation sites, the enhancing effect will overwhelm the depressing effect, thus, resulting in a higher crystallization rate. In addition, under the conditions of similar fiber surface nucleation density, due to the earlier nucleation and initi-

ate growth, the instantaneous nucleation case ($N_f = 20/\text{mm}$) crystallizes more quickly than the spontaneous case [Fig. 9(a), $\dot{N}_f = 1.2/\text{min/mm}$; Fig. 9(b), $\dot{N}_f = 20/\text{min/mm}$; and Fig. 9(c), $\dot{N}_f = 1000/\text{min/mm}$]. The increase of cooling rate leads to an acceleration of crystallization and a less obvious effect of nucleation density on fiber surface.

The observation in this section tells us that cooling rate and nucleation density on fibers are significant factors on the crystallization kinetics as well as the morphology. An increase of these two values causes an acceleration of crystallization and also a reduction of mean radius of spherulites. Moreover, the effect of instantaneous nucleation on fibers is more important than the spontaneous case under the conditions of same nucleation density on fibers.

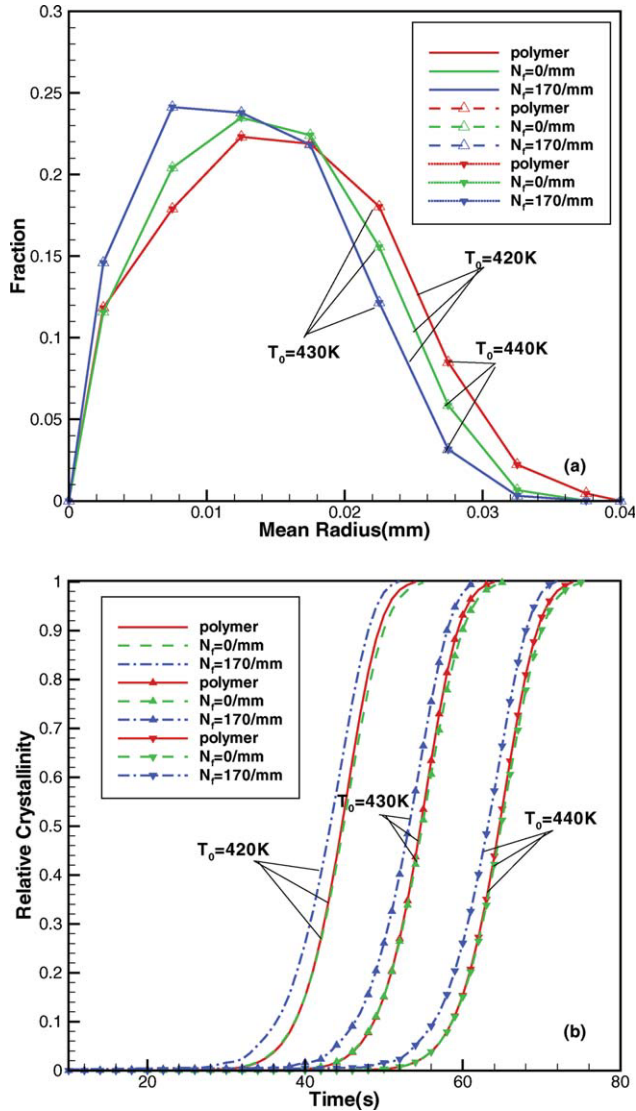


Figure 10 Effects of initial temperature on the mean radius of spherulites and crystallization rate. [Color figure can be viewed in the online issue, which is available at wileyonlinelibrary.com.]

Effects of initial temperature T_0

To explore the thermal history, the effect of initial temperature on the crystal morphology and the crystallization rate is studied, which is shown in Figure 10 where the cooling rate is set to be $c = 60\text{K}/\text{min}$. We test two extreme cases, namely, fiber serving no nucleation sites ($N_f = 0/\text{mm}$) and a great many of nucleation sites ($N_f \approx 170/\text{mm}$, with the nucleation rate per unit fiber surface $\dot{N}_f = 200/\text{min}/\text{mm}$). It is observed that in both cases the initial temperature has almost no effect on the mean radius of spherulites in the polymer bulk but has a drastic effect on the crystallization kinetics. As we expected, the decrease in the initial temperature leads to an acceleration of the crystallization and conversely.

Effects of fiber area fraction A_f

Effects of fiber area fraction on the crystallization in the nonisothermal system are discussed. Similar to the previous work in the isothermal system, we change the fiber area fraction $A_f (= l \cdot d \cdot n_f)$ through varying the amount of fiber number per area n_f while keeping the other parameters the same. Three cases are studied, namely, $n_f = 37.5, 46.9, 56.3/\text{mm}^2$, and the corresponding fiber area fractions are $A_f = 5.0\%, 7.5\%, 9.0\%$.

The effects of fiber area fraction on the mean radius of spherulites in the polymer bulk and the crystallization rate with the cooling rate $c = 60\text{K}/\text{min}$ are shown in Figure 11. In the case of fiber providing no surface nucleation, the increase of fiber area fraction leads to a larger space occupied by fibers

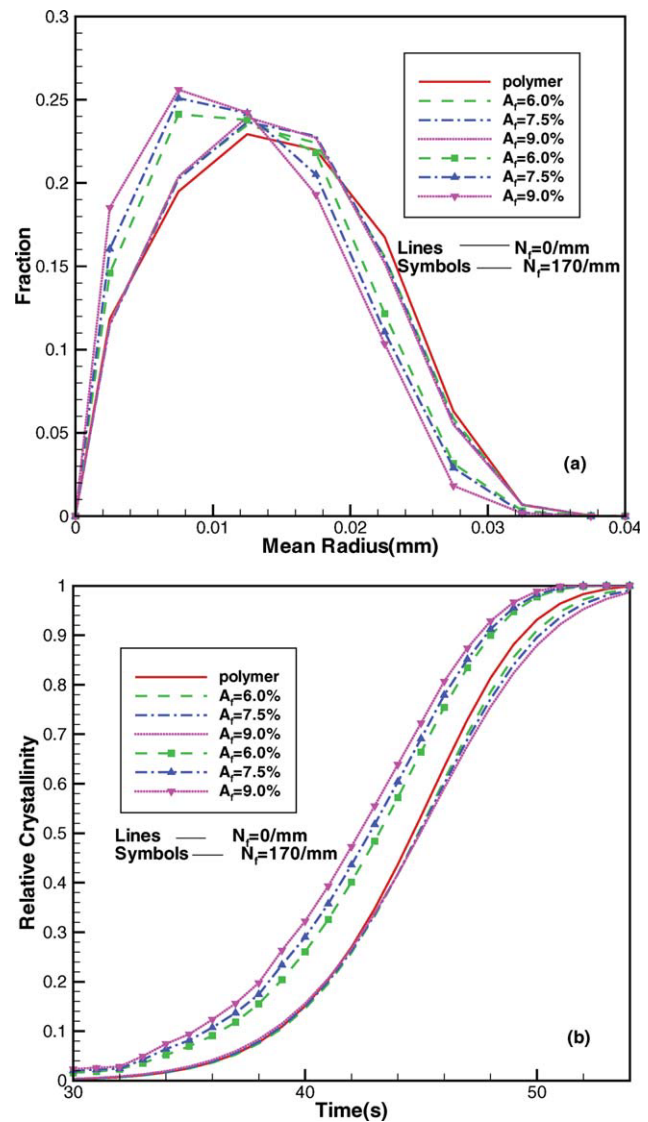


Figure 11 Effects of fiber area fraction on the mean radius of spherulites and crystallization rate. [Color figure can be viewed in the online issue, which is available at wileyonlinelibrary.com.]

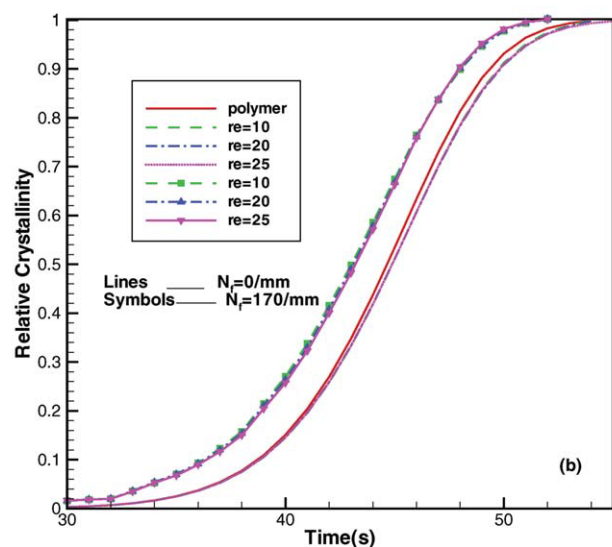
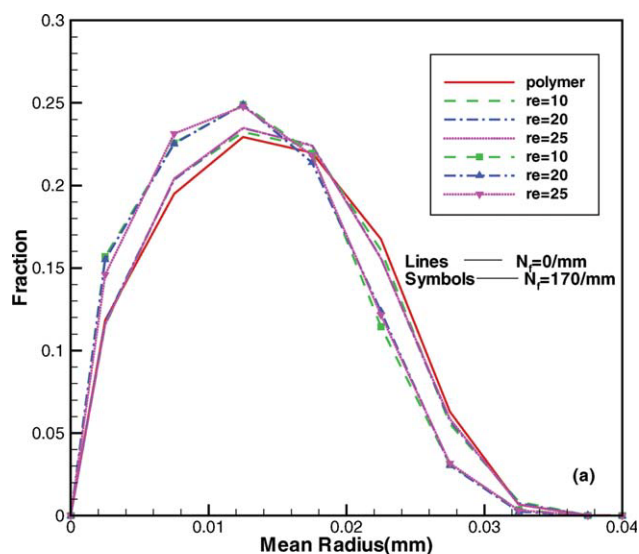


Figure 12 Effects of fiber length on the mean radius of spherulites and crystallization rate. [Color figure can be viewed in the online issue, which is available at wileyonlinelibrary.com.]

which hindering the spherulite growth front, therefore, the mean radius of spherulites and the corresponding crystallization rate are depressed monotonously. However, in the case of fiber serving a great many of surface nucleation sites, the increase of fiber area fraction leads to a increase of fiber surface (surface nucleation sites), hence, the mean radius of spherulites decreases dramatically and the crystallization rate accelerate strongly. This agrees with the experimental data of Zheng et al.² in the nonisothermal case as well as the numerical data of our pervious work in the isothermal case.

Effects of fiber size

Effects of fiber length are studied. Similar to the isothermal case, we test three cases, namely, $l = 80$,

160, and 200 μm . Defining the fiber aspect ratio as $re = l/d$ and holding the fiber diameter as $d = 8 \mu\text{m}$, the cases we studied become $re = 10, 20, 25$. Results are shown in Figure 12 in which the cooling rate and the fiber area fraction are set to be $c = 60\text{K}/\text{min}$ and $A_f = 6.0\%$, respectively. The calculations show that the effects of fiber length on both mean radius of spherulites and the crystallization rate are minor.

Effects of fiber diameter are also investigated. Three cases are studied, namely, $d = 20, 10, 8 \mu\text{m}$. Fixing the fiber length as $l = 200 \mu\text{m}$, the fiber aspect ratio we used in the study are $re = 10, 20, 25$. Figure 13 shows the effect of fiber diameter on the mean radius of spherulites and the crystallization rate. When no fiber surface nucleation sites is considered, the change of fiber diameter affects neither mean radius of spherulites nor the crystallization rate.

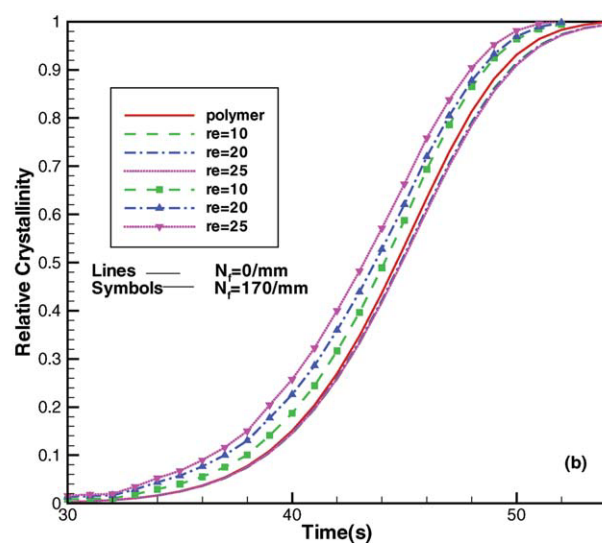
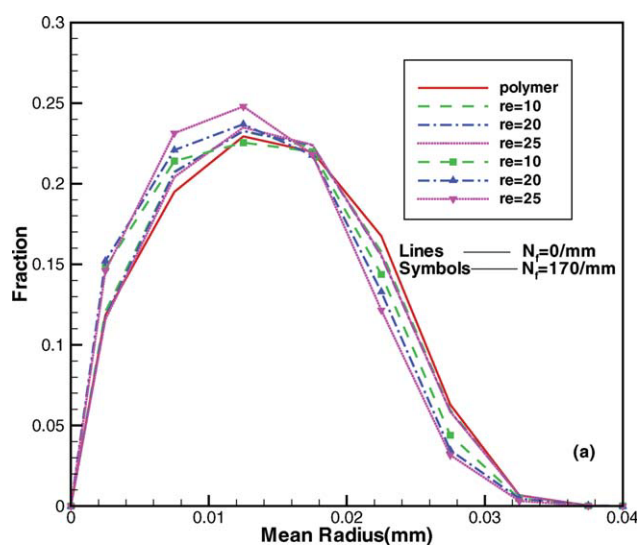


Figure 13 Effects of fiber diameter on the mean radius of spherulites and crystallization rate. [Color figure can be viewed in the online issue, which is available at wileyonlinelibrary.com.]

Nevertheless, when a great many of fiber surface nucleation sites is considered, the increase of fiber aspect ratio (decrease of fiber diameter) leads to the increase of fiber surface (surface nucleation sites), thus, the mean radius of spherulites decreases obviously and the crystallization rate is also enhanced significantly.

Roles of fiber size on the crystallization in the nonisothermal case are also similar to the isothermal one.

CONCLUSIONS

Computer simulation of crystallization kinetics and morphology in short fiber reinforced composites is presented in this article. The pixel coloring method is extended to the study of nonisothermal crystallization simulation. Results obtained in the polymer system show fair agreement with the Kolmogorov model. Moreover, results presented in the reinforced system also show qualitative agreement with the experimental and numerical data. Therefore, this method is reliable and valid in this study.

A parametric study is used to explore the influences of thermal condition and fibers on the crystallization in the reinforced system. We show the effects of cooling rate, initial temperature, fiber nucleation density, fiber content, fiber length, and fiber diameter on the crystallization. The results show that cooling rate is a significant factor to the crystallization kinetics as well as the morphology. In the case of higher cooling rate, the range of temperature for crystallization is wider which leads to a high nucleation density in polymer bulk and results in a reduction of mean size of crystals. The initial temperature only affects the crystallization kinetics and has minor impact on the morphology. The decrease in the initial temperature leads to an acceleration of the crystallization. Similar as the isothermal case in short fiber reinforced system, fibers in nonisothermal case also have a dual effect: fibers depress the crystallization rate when compared to the neat polymers or accelerate the crystallization rate by providing nucleation sites. The constraining effect is mainly depend-

ent on fiber content, whereas the enhancing effect is mainly determined by fiber surface and fiber nucleation density as well as surface nucleation mode.

We present a computer simulation for nonisothermal crystallization in short fiber reinforced system. We hope that the results presented in this study will provide useful suggestions for the modelization of the crystallization in short fiber reinforced system, and will give more insight about the crystallization in the industrial processes.

References

1. Run, M. T.; Song, H. Z.; Yao, C. G.; Wang, Y. J. *J Appl Polym Sci* 2007, 106, 868.
2. Zheng, L. J.; Qi, J. G.; Zhang, Q. H.; Zhou, W. F.; Liu, D. *J Appl Polym Sci* 2008, 108, 650.
3. Krause, T. H.; Kalinka, G.; Auer, C.; Hinrichsen, G. *J Appl Polym Sci* 1994, 51, 399.
4. Benard, A.; Advani, S. G. *J Appl Polym Sci* 1998, 70, 1677.
5. Piorkowska, E. *Macromol Symp* 2001, 169, 143.
6. Mehl, N. A.; Rebenfeld, L. *J Polym Sci Part B: Polym Phys* 1993, 31, 1677.
7. Mehl, N. A.; Rebenfeld, L. *J Polym Sci Part B: Polym Phys* 1993, 31, 1687.
8. Mehl, N. A.; Rebenfeld, L. *J Polym Sci Part B: Polym Phys* 1995, 33, 1249.
9. Nakamura, K.; Katayama, K.; Amano, T. *J Appl Polym Sci* 1973, 17, 1031.
10. Nakamura, K.; Watanabe, T.; Katayama, K.; Amano, T. *J Appl Polym Sci* 1972, 16, 1077.
11. Kolmogorov, A. N. *Bull Akad Sci USSR Class Sci Math Nat* 1937, 1, 355.
12. Avrami, M. *J Chem Phys* 1939, 7, 1103.
13. Avrami, M. *J Chem Phys* 1940, 8, 212.
14. Avrami, M. *J Chem Phys* 1941, 9, 177.
15. Charbon, C.; Swaminarayar, S. *Polym Eng Sci* 1998, 38, 644.
16. Huang, T.; Kamal, M. R. *Polym Eng Sci* 2000, 40, 1796.
17. Shen, C.; Zhou, Y.; Chen, J.; Li, Q. *Polym-Plast Tech* 2008, 47, 708.
18. Ruan, C.; Ouyang, J.; Liu, S.; Zhang, L. *Comput Chem Eng* 2011, Doi:10.1016/j.compchemeng. 2010.11.011.
19. Pantanin, R.; Coccoorullo, I.; Speranza, V.; Titomanlio, G. *Prog Polym Sci* 2005, 30, 1185.
20. Piorkowska, E.; Galeski, A.; Haudin, J. M. *Prog Polym Sci* 2006, 31, 549.
21. Pantanin, R.; Coccoorullo, I.; Speranza, V.; Titomanlio, G. *Polymer* 2007, 48, 2778.
22. Hoffman, J. D.; Miller, R. L. *Polymer* 1997, 38, 3151.
23. Charbon, C.; Rappaz, M. *Acta Mater* 1996, 44, 2663.